引用格式：ZHONG Guiming, HAN Xiaoshuai, ZHANG Xin, et al. Fabrication and Characterization of Deformable Mirror Driven by Piezoelectric Unimorph Actuator Array[J]. Acta Photonica Sinica, 2022, 51(1):0151125
钟贵明,韩小帅,张昕,等.单压电执行器阵列驱动的变形镜的制备与表征[J].光子学报,2022,51(1):0151125

单压电执行器阵列驱动的变形镜的制备与表征

钟贵明,韩小帅,张昕,娄军强,马剑强
(宁波大学 机械工程与力学学院,浙江 宁波 315211)

摘　要:为降低压电执行器阵列式变形镜的成本,提出了一种由单压电执行器阵列驱动的低成本变形镜。制备了19单元50 mm口径的变形镜样机,建立了基于Shack-Hartmann传感器的自适应光学测试系统,并对单个执行器性能、校正性能、镜面校平性能、变形镜频率响应特性进行了表征。测试结果显示,制备的变形镜单个执行器在50 V电压下波前变形量可达10 μm,可精确重构前14项Zernike多项式像差,校平后远场光斑接近艾里斑,变形镜一阶固有频率约为1.8 kHz。提出的单压电执行器阵列驱动的变形镜具有比较好的性能,在低成本自适应光学系统中具有应用前景。

关键词:变形镜;单压电执行器;自适应光学;波前像差;像差校正
中图分类号:TN384;O438　　**文献标识码**:A　　**doi**:10.3788/gzxb20225101.0151125

0　引言

自适应光学系统通过实时探测光学系统中的波面畸变,并控制变形镜镜面变形进行波前像差的补偿,使系统达到或接近衍射极限,在天文成像[1]、视觉科学[2]和高能激光器[3]等领域中发挥重要的作用。变形镜是自适应光学系统中的核心器件,其性能直接决定了系统的波前校正能力。基于压电材料驱动的变形镜因其优异的驱动性能,是目前较为常用的一类变形镜。其大致可分为两大类,一类为压电执行器阵列式变形镜,其由离散的压电执行器阵列通过连接柱推动薄镜面变形[4-6],主要用于致动器数目要求多且对校正带宽要求较高的场合;另一类为双压电片变形镜,由一层或多层压电层和镜面层粘接组成,利用压电材料的横向压电效应带动镜面产生弯曲变形[7-9],具有较高的交联值,对低阶像差校正能力较强。传统的压电执行器阵列式变形镜采用堆栈式执行器驱动,具有变形量大、谐振频率高的特点,但价格昂贵限制了其应用[10]。

中国中科院成都光电技术研究所和美国Xinetics公司等[11-12]通过改进执行器结构,采用横向压电效应的执行器结构形式,提升了变形镜的执行器密度,促进了整体系统设计的紧凑化,但是制作过程比较复杂,主要应用于天文领域。为了降低成本,荷兰OKO公司[13]提出了一种压电陶瓷管驱动的变形镜,陶瓷管执行器比传统的堆叠执行器成本更低,但价格仍然较高。此外,YANG E H和马剑强等[14-15]分别提出了基于压电薄膜和压电厚膜的微压电执行器阵列驱动的变形镜,具有驱动电压低、行程大的优点,但采用微加工工艺进行变形镜的制造,制造工艺比较复杂,尚处于原理样机阶段。

本文提出了一种具有大行程、低驱动电压、低成本的单压电执行器阵列驱动的变形镜,制备了19单元变形镜样机,搭建了基于Shack-Hartmann传感器的自适应光学测试系统,并对变形镜执行器性能、校正性能、镜面校平性能和频率响应特性等进行表征,证明其具有较好的性能,在低成本自适应光学系统中具有一定的应用前景。

基金项目:国家自然科学基金(No.51805280),工业控制技术国家重点实验室开放课题(No.ICT2021B44),浙江省省属高校基本科研业务费专项资金(No.SJLY2020002)
第一作者:钟贵明(1996—),男,硕士研究生,主要研究方向为压电变形镜的设计与制备。Email:1582922819@qq.com
导师(通讯作者):马剑强(1983—),男,副教授,博士,主要研究方向为压电器件、变形镜和自适应光学技术。Email: majianqiang@nbu.edu.cn
收稿日期:2021-09-05;**录用日期**:2021-11-04

1 结构与原理

单压电执行器阵列驱动的变形镜结构原理如图1所示，包括镜面、单压电片执行器阵列、连接柱和基座。单压电执行器阵列由多个固定在基座通孔上的单压电执行器组成，呈六边形排列。每个单压电执行器通过连接柱与镜面相连。单压电执行器由压电圆片和铜圆片构成，压电片的两面均覆盖电极层。当给单压电执行器施加电压时，由于横向压电效应执行器产生弯曲变形，执行器中心离面位移通过固定在单压电执行器中心的连接支柱传递到镜面，使镜面产生变形。当多个单压电执行器共同作用，可使镜面产生与畸变波前相共轭的形状，实现对波前像差的校正，相关设计工作参见文献[16]。

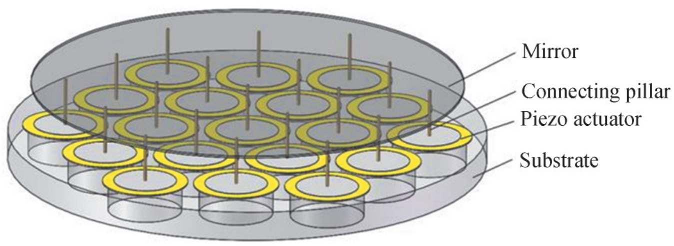

图1变形镜结构图

Fig.1 Structure of deformable mirror

2 制备流程

执行器采用的是商用的单压电执行器（FT-15T-4.4A1-2，苏州攀特电陶股份科技有限公司），由黄铜片和压电陶瓷片粘接而成，直径分别为15 mm和11 mm，厚度分别为80 μm和70 μm，其成本为传统压电执行器的十分之一。基座材料采用光学石英玻璃，带有19个通孔。镜面采用厚度350 μm的3英寸（1英寸=2.54 cm）单抛硅片（苏州晶硅科技有限公司），硅片表面未进行镀膜处理，后续可以根据实际应用要求进行镀膜。首先将19个单压电执行器与基座上的通孔同轴粘接，之后借助定位板将直径0.45 mm、长8 mm的铜支撑柱粘接在镜面的对应位置。接着镜面通过连接支柱和单压电执行器阵列同轴粘接。最后通过漆包线引出电极并焊接在电路板上，完成电气部分连接后进行变形镜的整体封装。制备的19单元单压电执行器阵列驱动的变形镜样机如图2所示，有效口径50 mm。由于所用材料均为通用材料，且制作方法相对简单，其成本远低于其他类型的压电执行器阵列式变形镜（特别是叠堆式压电变形镜）。

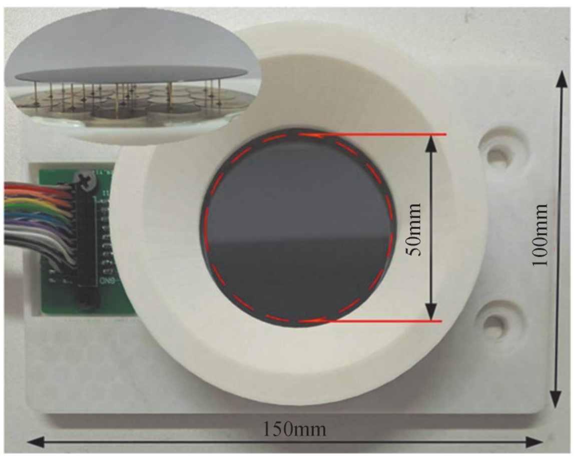

图2 变形镜实物

Fig.2 Prototype of the deformable mirror

3 性能表征

3.1 测试系统

为了验证单压电执行器阵列驱动变形镜的校正性能，搭建了基于Shack-Hartmann传感器的自适应光学

测试系统,如图3所示。激光器为半导体激光器(Thorlabs HLS635),是单模光纤输出波长为635 nm的红色激光。激光束首先通过分光棱镜进行分光,50%光束到达焦距为400 mm的透镜L1,经其准直后,输出的平行光到达变形镜。光束经镜面反射后原路返回再次经过分光棱镜BS1,50%光束90°方向反射透过透镜L2,透镜L1、L2组成10倍缩束系统(f_1=400 mm,f_2=40 mm)。最后,缩束后的光束经过分光镜BS2,50%光束由波前传感器(Thorlabs WFS150-7AR)接收,采用33×33阵列微透镜进行测量,并采用65项Zernike多项式进行波前像差拟合。波前传感器实时测得变形镜的波前信息并反馈给控制系统,从而控制变形镜生成目标面形。另外50%光束经过焦距为f_3=200 mm的透镜L3聚焦,其远场光斑由CCD相机采集。

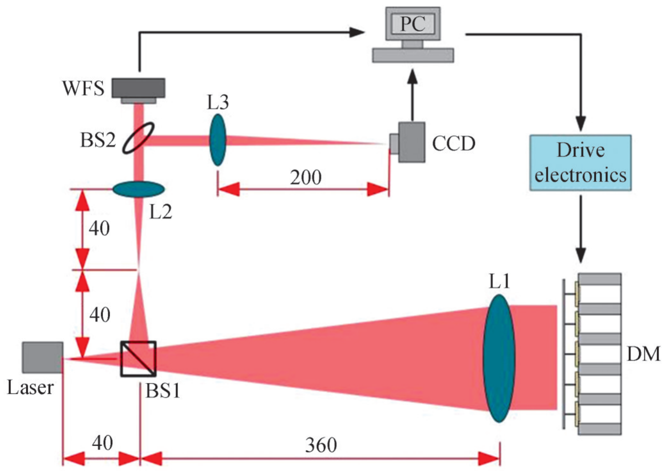

图3 自适应光学测试系统

Fig.3 Adaptive optics test system

3.2 执行器性能

单个执行器的性能对变形镜的整体性能有很大的影响,在50 V电压下实测得到的变形镜典型执行器的影响函数如图4所示。在50 mm有效口径下测得波前变形量的峰谷值(Peak-to-Valley,PV)分别为8.8 μm、10.6 μm、8.6 μm、9.9 μm。对1号执行器变形取截面分析得到中心执行器与相邻执行器之间的交联值约为25.4%,与林旭东等[17]研制的堆栈式压电变形镜23%的交联值接近。由此可知,该变形镜具有较大的变形量,且交联值较为合理(根据CILAS公司的变形镜设计经验,为了获得较好的校正性能,交联值10%~30%

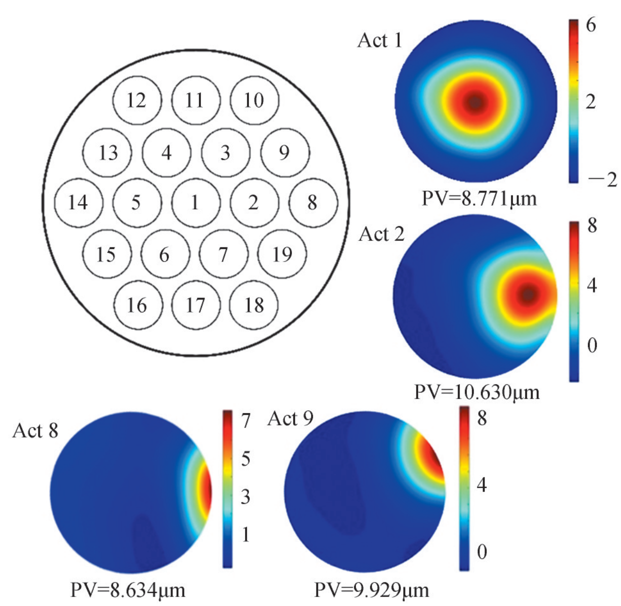

图4 典型执行器影响函数

Fig.4 Influence function of typical actuators

较为合理[18]),有利于像差的校正。

3.3 校正性能

为了验证变形镜的校正性能,依次实验重构了前14项Zernike多项式像差(除倾斜项外),并计算每个实际重构的Zernike多项式像差面型的PV值和均方根值(Root-Mean-Square,RMS),残余误差实测面型与理论面型之差,残余误差的均方根值记为ERR。实测的第3~14项Zernike多项式像差如图5。随着像差阶数增大,其重构幅值逐渐减小,其中重构像散像差(Z_3和Z_5)的PV约为7.5 μm,归一化的残余波前误差(ERR与RMS值之比)约为3.7%;重构离焦像差(Z_4)的PV约为3 μm,归一化的残余波前误差小于6.1%;重构三叶草像差(Z_6和Z_9)的PV约为4.4 μm,归一化的残余波前误差约为7.1%;重构彗形像差(Z_7和Z_8)的PV约为2.5 μm,归一化的残余波前误差约为10.3%。结果表明该变形镜对前9项Zernike多项式像差具有良好的重构能力,对Z_{10},Z_{14}项Zernike多项式像差具有一定的重构能力。该变形镜的执行器数目可进一步增加,这将会进一步提高其校正能力。

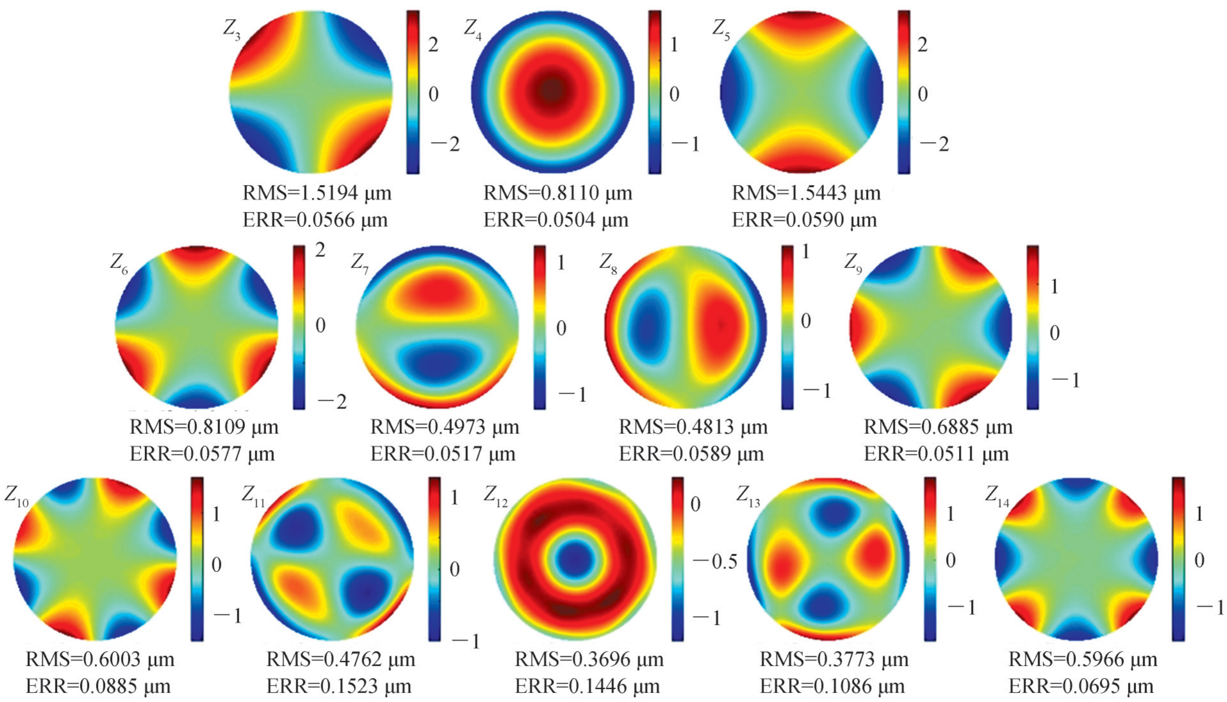

图5 重构前14项Zernike多项式像差

Fig.5 Reconstruction of the first 14 Zernike polynomial aberrations

3.4 镜面校平

变形镜样机的初始镜面形貌及校平后形貌如图6所示。由于变形镜在粘接的过程中无法避免地产生固化应力,且镜面较薄,导致与支撑柱粘接处的镜面质量下降,初始镜面存在像差,且初始镜面质量主要受低阶像差影响,校平后面型的波前PV值降为0.608 μm,对应的均方根值RMS为0.085 μm。校平后所剩像差为高阶像差,与支撑柱粘接应力有关,后续将进一步完善制备工艺,解决大口径高平整薄镜面的制备难题。

用CCD采集校平前后的远场光斑,结果如图7所示,由于校正前光斑强度很弱,所需曝光时间远大于校正后的曝光时间。校平前,焦斑由于存在较大的波前畸变,形状发生畸变;镜面校平后,光斑接近艾里斑,这意味着系统中的大部分像差可以很好地被变形镜校正。光斑边缘有部分杂散斑,这是由于19单元执行器的变形镜校正能力受限,无法校正高阶像差导致。

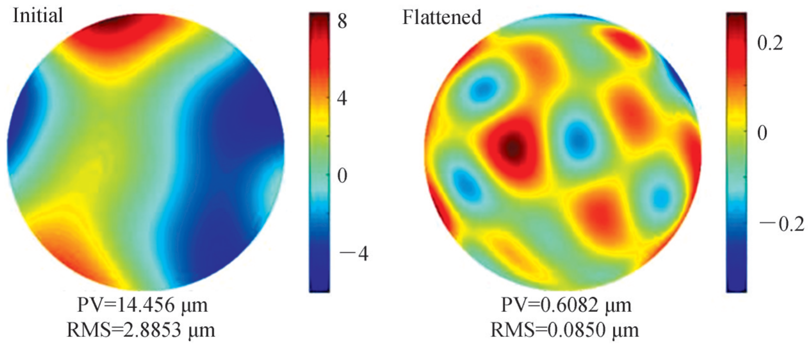

图 6　初始与校平后镜面形貌

Fig.6　Initial and flattened mirror surface

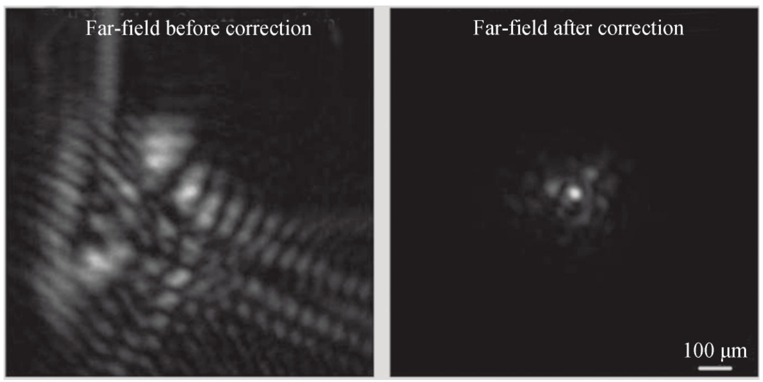

图 7　镜面校正前后远场光斑

Fig.7　The far-field spot before and after correction

3.4　频率响应特性

为测量单压电执行器阵列驱动的变形镜的频率响应,通过信号发生器给变形镜中心执行器施加 5 V 不同频率的正弦信号,使镜面产生变形,进而带动相邻执行器产生变形,由于压电效应,用示波器测量其上的电压,电压值大小反映了镜面的振动响应情况。结果如图 8 所示,在低频部分响应曲线较为平稳,当频率达到了 1.8 kHz 时产生第一个共振峰,当频率达到 2.1 kHz 时产生第二个共振峰,表明制备的单压电执行器阵列驱动变形镜具有比较高的固有频率。

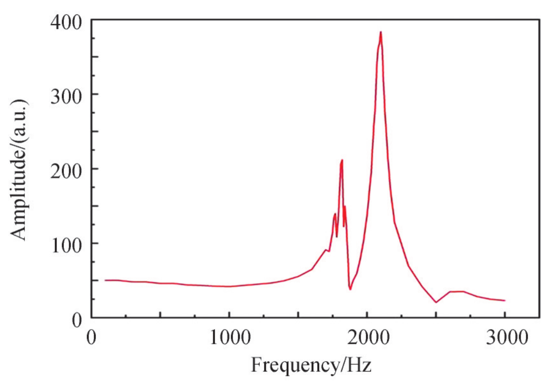

图 8　变形镜频率响应特性

Fig.8　Frequency response characteristics of deformable mirror

4 结论

针对压电驱动变形镜所存在的成本高、制作复杂等问题，提出了一种单压电执行器阵列驱动的变形镜。制备了19单元变形镜样机，为了测试变形镜的性能，建立了一种基于Shack-Hartmann传感器的自适应光学测试装置并进行测试，测试结果表明制备的变形镜单个执行器在50 V电压下波前变形量可达10 μm，能够精确重构典型低阶Zernike多项式像差，镜面校平后残余误差可达到0.085 μm，在系统像差被校正后获得了接近艾里斑的远场光斑。此外，频率响应测试显示其一阶固有频率可达1.8 kHz。与传统压电执行器阵列式变形镜相比，该变形镜具有行程大、工作电压低、成本低的特点。该变形镜的执行器数目可进一步增加，作为大口径高执行器数目变形镜的一种实施方案。目前该设计的初始镜面平整度还有待进一步提高，在一定程度上限制了镜面的校平性能，后续将进一步完善制备工艺，解决大口径高平整薄镜面的制备难题，未来有望在低成本自适应光学领域甚至在天文成像中获得应用。

参考文献

[1] WANG Hairen. Research on a bimorph piezoelectric deformable mirror for adaptive optics in optical telescope[J]. Optics Express, 2017, 25(7): 8115-8122.

[2] WANG Yuanyuan, HE Yi, WEI Ling, et al. Bimorph deformable mirror based adaptive optics scanning laser ophthalmoscope for retina imaging in vivo[J]. Chinese Optics Letters, 2017, 15(12):121102.

[3] LI Guohui, XU Honglai, WU Jing, et al. Active correction of intracavity aberration combination in unstable resonator thin-disk laser[J]. Chinese Journal of Lasers. 2020, 47(10):30-37.
李国会，徐宏来，吴晶，等. 非稳腔薄片激光器腔内像差组合式主动校正技术[J]. 中国激光, 2020, 47(10):30-37.

[4] SUN Licheng, ZHENG Yamin, SUN Chuang, et al. Simulational and experimental investigation on the actuator-corresponding high-frequency aberration of the piezoelectric stacked array deformable mirror[J]. Optics Express, 2018, 26(18):23613-23628.

[5] CHEN Kai, CHEN Junjie, MAO Yuxin, et al. Simulation and experiment of 214-element unimorph deformable mirror with edge-driven[J]. Acta Photonica Sinica, 2016, 45(8):0822004.
陈凯，陈俊杰，毛宇昕，等. 带边缘驱动的214单元单压电变形镜仿真与实验[J]. 光子学报, 2016, 45(8):0822004.

[6] WLODARCZYK K L, BRYCE E, SCHWARTZ N, et al. Scalable stacked array piezoelectric deformable mirror for astronomy and laser processing applications[J]. Review of Scientific Instruments, 2014, 85(2):024502.

[7] MA Jianqiang, LIU Ying, HE Ting, et al. Double drive modes unimorph deformable mirror for low-cost adaptive optics [J]. Applied Optics, 2011, 50(29):5647-5654.

[8] PENG Tairan, LI Wenlai, LOU Junqiang, et al. Development of a bimorph deformable mirror driven by positive-voltage actuators at edge[J]. Acta Photonica Sinica, 2019, 48(8):0822003.
彭泰然，李文来，娄军强，等. 正电压边缘驱动的双压电片变形镜研制[J]. 光子学报, 2019, 48(8):0822003.

[9] TOPOROVSKIY V, TOPOROVSKIY A V, SAMARKIN V, et al. Bimorph deformable mirror with a high density of electrodes to correct for atmospheric distortions[J]. Applied Optics, 2019, 58(22):6019-6026.

[10] WEYRAUCH T, VORONTSOV M A, BIFANO T G, et al. Performance evaluation of micromachined mirror arrays for adaptive optics[C]. Proceedings of SPIE, 2000, 4124:41241.

[11] EALEY M A, TRAUGER J T. High-density deformable mirrors to enable coronographic planet detection[C]. SPIE, 2004, 5166:172-179.

[12] GUAN Chunlin, ZHANG Xiaojun, DENG Jianming, et al. Deformable mirror technologies at Institute of Optics and Electronics, Chinese Academy of Sciences[J]. Opto-Electronic Engineering, 2020, 47(10):200337.
官春林，张小军，邓建明，等. 中国科学院光电技术研究所的变形反射镜研究进展[J]. 光电工程, 2020, 47(10):200337.

[13] VDOVIN G, LOKTEV M, SIMONOV A. Low-cost deformable mirrors: technologies and goals[C]. Proceedings of the SPIE, 2005, 5894:58940B.

[14] YANG E H, HISHINUMA Y, CHENG Jiangong, et al. Thin-film piezoelectric unimorph actuator-based deformable mirror with a transferred silicon membrane[J]. Journal of Microelectromechanical Systems, 2006, 15(5):1214-1225.

[15] MA Jianqiang, LIU Ying, CHEN Caipeng, et al. Deformable mirrors based on piezoelectric unimorph microactuator array for adaptive optics correction[J]. Optics Communications, 2011, 284:5062-5066.

[16] TIAN Lei, ZHU Zhengxiong, ZHANG Jialian, et al. Design and fabrication of deformable mirror driven by piezoelectric buzzer array[C]. Proceedings of the SPIE, 2017, 10255:102555F.

[17] LIN Xudong, LIU Xinyue, WANG Jianli, et al. Developement and performance test of the 961-element deformable mirror[J]. Acta Optica Sinica, 2013, 33(6):0601001.
林旭东，刘欣悦，王建立，等. 961单元变形镜研制及性能测试[J]. 光学学报, 2013, 33(6):0601001.

[18] SINQUIN J, LURCON J, GUILLEMARD C, et al. Deformable mirror technologies for astronomy at CILAS[C]. SPIE Astronomical Telescopes + Instrumentation, 2008, 7015:70150O.

Fabrication and Characterization of Deformable Mirror Driven by Piezoelectric Unimorph Actuator Array

ZHONG Guiming, HAN Xiaoshuai, ZHANG Xin, LOU Junqiang, MA Jianqiang
(*Faculty of Mechanical Engineering and Mechanics, Ningbo University, Ningbo, Zhejiang* 315211, *China*)

Abstract: Adaptive optics system can detect the wavefront distortion of the optical system in real time and then control the mirror deformation of a deformable mirror to compensate the wavefront aberrations, so that the optical system can reach or approach the diffraction limit. It plays an important role in the fields of astronomical imaging, visual science and high-energy laser. Deformable mirrors driven by piezoelectric materials are widely used in the adaptive optics systems due to their high driving force and fast response. Piezoelectric deformable mirrors can be divided into two categories. One is the piezoelectric actuator array deformable mirror which is driven by the discrete piezoelectric actuators through the connecting pillars to deform the thin mirror. It is mainly used for the applications which require high number of actuators and high correction bandwidth. The other one is the bimorph deformable mirror which is composed of one or more piezoelectric layers bonded with the mirror layer. The transverse piezoelectric effect of piezoelectric materials is used to drive the mirror to produce bending deformation. Bimorph deformable mirror has a high interactuator coupling value and a strong correction capability for low-order aberrations. The traditional piezoelectric actuator array deformable mirror is driven by stack piezoelectric actuators, which has the advantages of large deformation and high resonant frequency. However, the high price limits its applications. Chengdu Institute of Optoelectronics Technology of Chinese Academy of Sciences and Xinetics Company improved the actuator structure with transverse piezoelectric effect to improve the actuator density of the deformable mirror and promote the compactness of the overall system design. However, the manufacturing process is complicated and is mainly applied in the astronomical field. In order to reduce the cost, OKO Technologies has proposed a deformable mirror driven by piezoelectric ceramic tubes which are cheaper than traditional stacked actuators. The price is still expensive. In addition, YANG E H and Ma Jianqiang proposed a deformation mirror driven by piezoelectric thin film and piezoelectric thick film array of micro-piezoelectric actuators, respectively. These deformable mirrors have the advantages of low drive voltage and large stroke. However, the manufacturing process of such deformation mirrors using micro-machining technology is complicated. This kind of deformation mirror is still in the stage of principle prototype. In order to further reduce the cost of deformable mirror with piezoelectric actuator array, a low-cost deformable mirror driven by piezoelectric unimorph actuator array is proposed in this paper. The deformable mirror comprises a mirror, a piezoelectric unimorph actuator array, connecting pillars and a substrate. The piezoelectric unimorph actuators are hexagonally arranged on the substrate with corresponding through holes. The piezoelectric unimorph actuator consists of a copper layer and a piezoelectric layer with both sides covered by electrodes. When a voltage is applied to the piezoelectric actuator, the actuator bents due to the transverse piezoelectric effect. The out of plane displacement of the actuator is transmitted to the mirror through the connecting pillar fixed at the center of the piezoelectric unimorph actuator, resulting in the deformation of the mirror. When all the piezoelectric actuators work together, the mirror can produce a conjugate shape with the distorted wavefront to compensate the wavefront aberrations. A deformable mirror prototype with 19 actuators and an effective pupil of 50 mm was fabricated. The piezoelectric unimorph actuator is commercially available, which is made of a brass disc and a piezoelectric ceramic disc bonded together with the diameters of 15 mm and 11 mm, and the thickness of 80 μm and 70 μm, respectively. The substrate material is optical quartz glass with 19 through holes. The mirror is a 3-inch single crystal silicon wafer with a thickness of 350 μm. Since the materials used are all commercially available and the manufacturing process is relatively simple, the cost of the proposed deformable mirror is much lower than other types of piezoelectric actuator array deformable mirrors (especially the stacked piezoelectric deformable mirrors). In order to verify the performances of deformable mirror driven by piezoelectric unimorph actuator array, an adaptive optics test system based on Shack-Hartmann sensor is built. A microlens array with 33×33 lenses is used for the measurement. Sixty-five Zernike polynomials are used for wavefront aberration fitting. The characteristics of actuator stroke, correction performance, mirror performance and frequency response are performed experimentally. The experimental results show that the wavefront deformation of a single actuator of the fabricated deformable mirror can reach 10 μm under a voltage of 50 V. The deformable mirror can accurately reconstruct the first 14-term Zernike polynomial aberrations. The far-field spot after correction is close to the Airy disc. The first-order natural frequency of the deformable mirror can reach 1.8 kHz. Compared to the traditional piezoelectric actuator array deformation mirror, this deformation mirror has the advantages of large stroke, low working voltage and low cost. The actuator number can be further increased for the implementation of the deformation mirror with large diameter and high number of actuators. The proposed deformable mirror has a promising application in the low-cost adaptive optics systems and even in astronomical imaging applications.

Key words: Deformable mirror; Piezoelectric unimorph actuator; Adaptive optics; Wavefront aberration; Aberration correction

OCIS Codes: 010.1080; 220.1080; 230.0230

Foundation item: National Natural Science Foundation of China (No. 51805280), Open Project of State Key Laboratory of Industrial Control Technology (No. ICT2021B44), Basic Scientific Research Funds of Zhejiang Provincial Universities (No. SJLY2020002)